Morphology, biochemistry and pathophysiology of MENX-related pheochromocytoma recapitulate the clinical features

Tobias Wiedemann[1], Mirko Peitzsch[2], Nan Qin[2], Frauke Neff[3], Monika Ehrhart-Bornstein[4], Graeme Eisenhofer[2,4], Natalia S. Pellegata[1]

[1]Institute for Diabetes and Cancer, Helmholtz Zentrum München, Ingolstaedter Landstrasse 1, 85764 Neuherberg, Germany; [2]Institute of Clinical Chemistry and Laboratory Medicine, University Hospital Carl Gustav Carus, Medical Faculty Carl Gustav Carus, Technische Universität Dresden, Fetscherstraße 74, 01307 Dresden, Germany; Department of Internal Medicine III, University Hospital Carl Gustav Carus, Technische Universität Dresden, Fetscherstraße 74, 01307 Dresden, Germany; [3]Institute of Experimental Genetics, Helmholtz Zentrum München, Ingolstaedter Landstrasse 1, 85764 Neuherberg, Germany; [4]Division of Molecular Endocrinology, Medical Clinic III, Technische Universität Dresden, Dresden, Germany.

Pheochromocytomas (PCCs) are tumors arising from neural crest-derived chromaffin cells. There are currently few animal models of PCC that recapitulate the key features of human tumors. Since such models may be useful for investigations of molecular pathomechanisms and development of novel therapeutic interventions, we characterized a spontaneous animal model (MENX rats) that develops endogenous PCCs with complete penetrance. Urine was longitudinally collected from wild-type (wt) and MENX-affected (mutant) rats and outputs of catecholamines and their O-methylated metabolites determined by mass spectrometry. Adrenal catecholamine contents, cellular ultrastructure and expression of phenylethanolamine N-methyltransferase (PNMT), which converts norepinephrine to epinephrine, were also determined in wt and mutant rats. Blood pressure was longitudinally measured and end-organ pathology assessed. Compared to wt rats, mutant animals showed age-dependent increases in urinary outputs of norepinephrine ($P=0.0079$) and normetanephrine ($P=0.0014$) that correlated in time with development of tumor nodules, increases in blood pressure and development of hypertension-related end-organ pathology. Development of tumor nodules, which lacked expression of PNMT, occurred on a background of adrenal medullary morphological and biochemical changes occurring as early as 1 month of age and involving increased adrenal medullary concentrations of dense cored vesicles, tissue contents of both norepinephrine and epinephrine and urinary outputs of metanephrine, the metabolite of epinephrine. Taken together, MENX-affected rats share several biochemical and pathophysiological features with PCC patients. This model thus provides a suitable platform to study the pathogenesis of PCC for preclinical translational studies aimed at development of novel therapies for aggressive forms of human tumors.

Pheochromocytomas (PCCs) and paragangliomas (PGLs) are rare neuroendocrine tumors derived from chromaffin cells of the adrenal medulla and paraganglia of the autonomic nervous system, respectively. PCCs/PGLs occur sporadically or as a result of an inherited germline mutation in one of at least 14 genes (35%–40% of cases), including *VHL*, *NF1*, *RET*, *SDHA*, *SDHB*, *SDHC*, *SDHD*, *SDHAF2*, *HIF2α*, *TMEM127*, *MAX*, *FH*, *PHD2 and MDH2* (1). Somatic mutations of several of the above genes also appear to be responsible sporadic PCC/PGL, in particular, activating mutations of *HIF2α*, are rare in the germline and occur mainly as somatic mutations. Re-

ISSN Print 0013-7227 ISSN Online 1945-7170
Printed in USA

Received February 19, 2016. Accepted May 11, 2016.

Abbreviations:

cently, integrative genomic approaches have identified other common alterations in sporadic PCC that now await functional validation (2, 3). Gene expression profiling of human PCC/PGL has demonstrated that transcriptomic signatures of these tumors reflect the underlying driver mutation (4, 5). Indeed, PCCs and PGLs can be divided into two main clusters, designated as Cluster 1 and Cluster 2; Cluster 1 comprises tumors having germline mutations in *VHL*, *SDHx*, *FH* and probably *HIF2α*, whereas Cluster 2 includes tumors associated with mutations in *NF1*, *RET*, *MAX*, and *TMEM127* as well as most of the sporadic cases (1).

Although usually benign, approximately 10% of PCC and 35% of PGL cases are malignant as defined by the presence of distant metastases (6). The first-line therapy for patients with localized disease is surgery (7). For patients with metastatic disease systemic conventional chemotherapy has been tested without clear benefit on overall survival. Radiotherapy with the radiopharmaceutical ^{131}I-meta-iodobenzylguanidine (^{131}I-MIBG) was shown to have positive therapeutic effects, but tumor regression occurred in only 30% of patients (8). Some targeted therapies have also been evaluated: treatment with the tyrosine kinase inhibitor, sunitinib, has shown some efficacy in patients with progressive disease (9), whereas the mTOR inhibitor everolimus had limited efficacy (10, 11). There thus remains considerable clinical need for more effective therapies against aggressive forms of this tumor entity.

Animal models of cancer have been instrumental to our understanding of disease progression and spread, in elucidating gene function and for identifying and testing novel therapeutic approaches. For rare tumors, such as PCC/PGL, having suitable animal models that are representative of the situation in patients is essential, particularly since obtaining large cohorts for molecular studies or clinical trials is a challenge. Transgenic mice developing PCC alone or in combination with other malignancies have been described, and include mice heterozygous for *Rb1* gene deletion (12), with the combined deletion of *Rb1* and *p53* (13), heterozygous for a loss-of-function mutation in *Nf1* (14), homozygous for the deletion of both p27 and p18 (15). Monoallelic inactivation of the tumor suppressor gene *PTEN*, alone or in combination with p27 inactivation, predisposes animals to bilateral PCC (16). Due to often incomplete tumor penetrance and phenotypic differences between engineered mouse strains and the corresponding human disease, these animal models have provided limited value for elucidating the molecular pathogenesis or evaluating antitumor agents against PCC/PGL.

Allograft and xenograft models of the mouse MPC 4/30/PRR (MPC) PCC cell line (17) and of its aggressive derivative MTT (mouse tumor tissue-derived) cell lines (18) have been established to evaluate the efficacy of novel compounds or to set up imaging protocols (19–21). These models have the limitation that the tumorigenic process is accelerated and not physiological.

The MENX multiple endocrine neoplasia (MEN) syndrome is a multitumor syndrome that spontaneously arose in a rat strain due to a germline homozygous mutation in p27. MENX-affected (mutant) rats develop endogenous bilateral PCCs with complete penetrance and with time-dependent progression from hyperplasia to tumor nodule formation (22). Rat PCCs share similarities with their human counterpart in terms of histo-pathological features, gene copy number variations (23), expression signatures (24) and uptake of radiolabeled tracers for imaging (25, 26). MENX rats may therefore provide a valuable tool to elucidate PCC tumorigenesis and to perform preclinical trials. Exploiting this PCC animal model for preclinical and translational studies requires not only comprehensive characterization of the underlying tumor biology, but also of the associated biochemical and pathophysiological features.

With the above in mind, we have further characterized MENX rats with a particular focus on key features in patients with PCCs, including catecholamine production, metabolism and secretion, chromaffin cell ultrastructure, blood pressure (BP) and end-organ pathological changes. We here report that MENX mutant rats show catecholamine-related biochemical features also observed in patients with PCCs. Affected rats further display elevated BP and morphological changes in the heart and kidneys similar in nature to those observed hypertensive patients. The similarities between the phenotypic features of MENX rats and patients with PCC indicate that this animal model provides a valuable tool to study tumorigenesis of adrenomedullary cells and from this develop new therapeutic strategies to target aggressive forms of PCC/PGL.

Materials and Methods

Animals

The features of the MENX rat strain have previously been reported (27). For all studies, male and female MENX-affected and wild-type Sprague–Dawley rats were group housed under controlled conditions (temperature 23°C, 12-hour light, 12-hour dark cycle). Animals had access to standard rodent chow (Fa. Altromin) and water ad libitum. All procedures were approved by local authorities (AZ 55.2–1–54-2532–225-13) and complied with German animal protection laws.

Biomaterial collection and processing

Homozygous mutant rats used in this study were sacrificed at 1, 2, 3, 4, 6 and 8 months of age, and wild-type littermates were

sacrificed in parallel for comparison. Immediately following euthanasia, trunk blood was removed and collected. All rats were inspected for the presence of macroscopically visible lesions, which were sampled, weighted and immersion fixed in 4% buffered formalin. Later they were embedded in paraffin. Similarly, relevant internal organs (ie, endocrine glands, liver, lung, heart, kidneys, spleen, thymus) were collected, fixed in formalin and embedded in paraffin. Urine was collected from wild-type and mutant rats at different ages and snap-frozen in liquid nitrogen. Samples were stored at −80 until analysis. Rat adrenal tissues were collected at necropsy, weighted, snap-frozen and stored at −80 until used.

Histology and immunohistochemistry

Formalin-fixed, paraffin-embedded tissues were sectioned (3 μm) and stained with hematoxylin and eosin (HE), periodic acid-Schiff (PAS) or Elastin-Van Gieson's trichrome according to established protocols. Immunohistochemistry (IHC) was performed on an automated immunostainer (Discovery XT® Ventana Medical Systems) as previously described (28). Staining of 3-μm rat tissue sections was performed with antibodies against phenylethanolamine N-methyltransferase (PNMT) (Enzo Life Science) (Table 1) (24). Images were recorded using a Hitachi camera HW/C20 installed in a Zeiss Axioplan microscope with Intellicam software (Zeiss MicroImaging). Stainings were reviewed by an experienced pathologist (F.N.).

Measurements of catecholamines and O-methylated metabolites

Urinary norepinephrine (NE), epinephrine (EPI), dopamine (DA), and their respective O-methylated metabolites, normetanephrine (NMN), metanephrine (MN) and 3-methoxytyramine (MTY), were determined by liquid chromatography with tandem mass spectrometry (LC-MS/MS) as previously described (29). In brief, analytes were extracted from urine by an offline solid phase extraction procedure and subsequently directly injected into the LC-MS/MS system. Intra-assay coefficients of variation were respectively determined at 7.1%, 10.3% and 5.1% for NE, EPI and DA, and 9.0%, 5.7% and 4.5% for NMN, MN and MTY. Concentrations were volume corrected using urinary creatinine excretion levels. Tissue catecholamines were measured by liquid chromatography with electrochemical detection (30).

Blood pressure measurements

Blood pressure and heart rate were measured by a noninvasive computerized tail-cuff method using the MC4000 Blood Pressure Analysis Systems (Hatteras Instruments, Cary, NC) (31). Measurements were carried out at 4, 6 and 8 months of age with 10 measurement runs in each session.

Ultrastructural analysis

For electron microscopy (EM), rat adrenomedullary fragments (~1 mm^3) collected at necropsy were fixed in 2.5% glutaraldehyde in 0.1 M sodium-cacodylate buffer pH 7.4 (Science Services, Germany), postfixed in 2% aqueous osmium-tetraoxide (pH 7.3), dehydrated in gradual ethanol (30%–100%) and propylene oxide, and embedded in epoxy resin. Semithin sections were cut and stained with toluidine blue. Ultrathin sections (70 nm) were contrasted with uranyl acetate and lead citrate and examined at 80 kV under a Philips (Electronic Instruments, Mahwah, NJ) electron microscope (EM) 301.

Statistical analysis

Statistical analyses used the JMP statistics software package (SAS Institute Inc, Cary, NC). Impact of genotype was established using multivariate analyses that included consideration of age with a longitudinal repeated measures design and additional correction for influence of gender. Results of the BP and tissue catecholamine measurements are shown as the mean ± SEM. A paired two-tailed Student's t test was used to detect significance between two series of data, and $P < .05$ was considered statistically significant.

Results

Urinary biochemistry of adult rats

A characteristic feature of functional PCCs is production and metabolism of catecholamines to their O-methylated metabolites within tumor. Dopamine is metabolized to methoxytyramine, norepinephrine to normetanephrine and epinephrine to metanephrine. Thus, measuring production of the metabolites, rather than the precursor catecholamines, provides the recommended approach for diagnosis. To determine whether PCCs in the rat MENX model show similar catecholamine-related biochemical features to humans, we analyzed a series of 11 homozygous mutant rats (4 males and 7 females) and 14 wild-type (wt) age-matched rats (8 males and 6 females) for their urine outputs of norepinephrine, epinephrine, dopamine, normetanephrine, metanephrine and 3-me-

Table 1. Antibody list

Protein name	Host	Company	Cat. #	Dilution
Phenylethanolamine N-methyltransferase (PNMT)	Rabbit	Enzo Life Science	BML-PZ1040−0050	1:500

thoxytyramine. Urine samples were collected consecutively from each animal at 4, 6 and 8 months of age.

Mutant rats at 3–4 months of age show adrenomedullary cell hyperplasia, which then progresses to PCC by 8 months of age (24). Using a statistical model considering gender and presence of mutations as independent variables and urinary outputs of amines as dependent repeated variables, we established that mutant rats show age-associated changes and differences in urinary outputs compared to wt animals, consistent with early adrenal medullary hyperplasia followed by the development of tumors (Figure 1). Specifically, mutant rats showed progressive increases in urinary outputs of norepinephrine ($P = .0079$), normetanephrine ($P = .0014$) and 3-methoxytyramine ($P < .0001$) with advancing age compared to wt animals. Urinary outputs of norepinephrine and normetanephrine were not different at 4 months but were more than 2-fold higher ($P < .002$) at 8 months of age, when all mutant animals showed PCCs at necropsy compared to the absence of neoplastic lesions in wt rats.

In contrast to norepinephrine and normetanephrine, urinary outputs of dopamine, epinephrine and metanephrine did not increase with advancing age in mutant vs wt rats (Figure 1). Urinary outputs of dopamine, methoxytyramine and metanephrine, but not epinephrine, were already significantly increased ($P < .01$) in mutant vs wt animals at 4 months of age, and remained elevated at 6 and 8 months. Urinary outputs of metanephrine in particular were over 2.5-fold higher in mutant than wt animals at all ages. Interestingly, epinephrine did not show the same pattern as its O-methylated metabolite, metanephrine, which showed no significant difference when compared to wt animals (Figure 1).

Biochemistry and morphology of young rats

Due to the pronounced increase in urinary outputs of metanephrine in 4-month-old mutant compared to wt rats, we extended our measurements of catecholamines and metanephrines to younger animals. We collected urine samples from nineteen 1-month-old mutant rats (11 females, 8 males) and from 9 age-matched wt littermates (5 females, 4 males) and measured catecholamines as reported above. The results showed that indeed metanephrine excretion is significantly higher ($P < .0001$) in mutant rats already at 1 month of age compared to wt rats (Figure 2A and 2B). In contrast, urinary outputs of the other metabolites and their precursor catecholamines were not significantly different among the two groups of animals at this age.

Additionally, we determined the amount of norepinephrine, epinephrine and dopamine in adrenal gland tissues of 1-month-old mutant (n = 4) and wt (n = 5) littermates. We established that the adrenal glands of mutant 1-month old rats contained higher relative total levels of

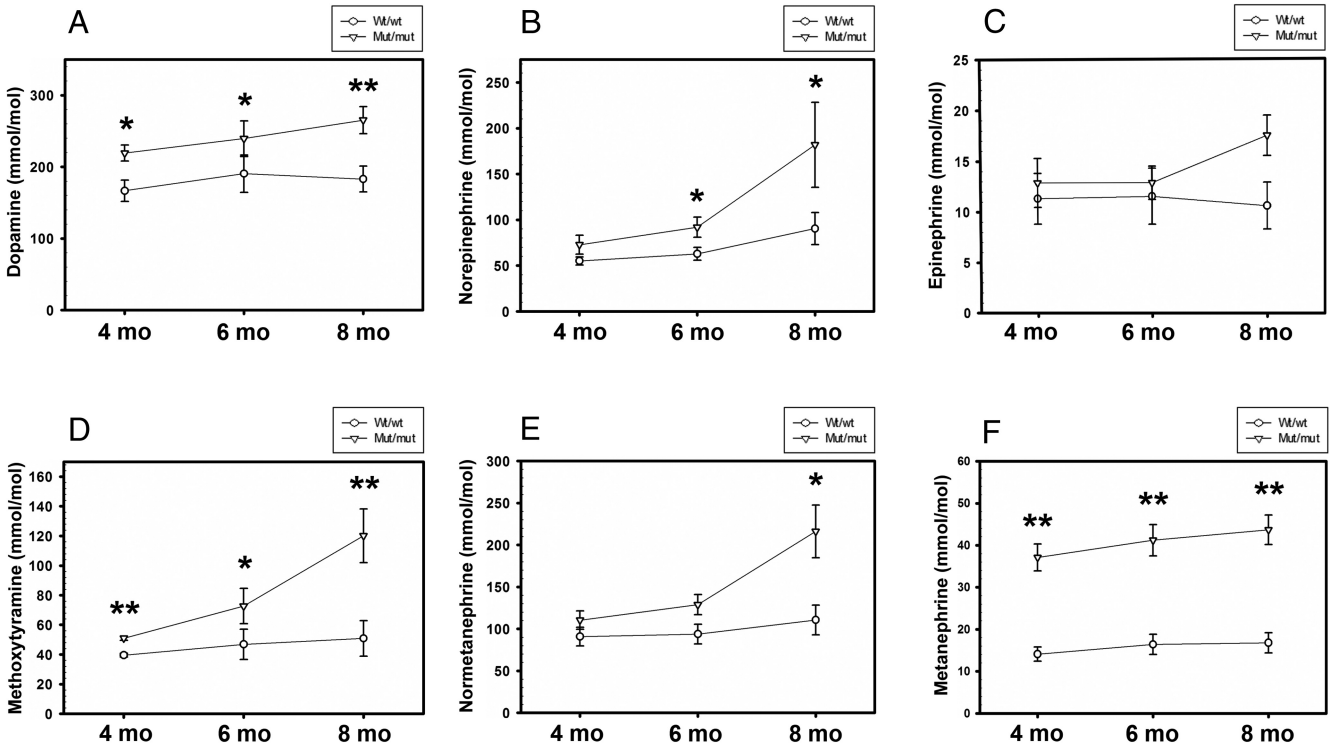

Figure 1. Longitudinal measurements of catecholamine levels in the urine of wild-type (Wt/wt) and homozygous mutant (Mut/mut) rats sampled at different ages. Eleven mutant and 14 wild-type rats were analyzed. Mo, months; *, $P < .05$; **, $P < .001$.

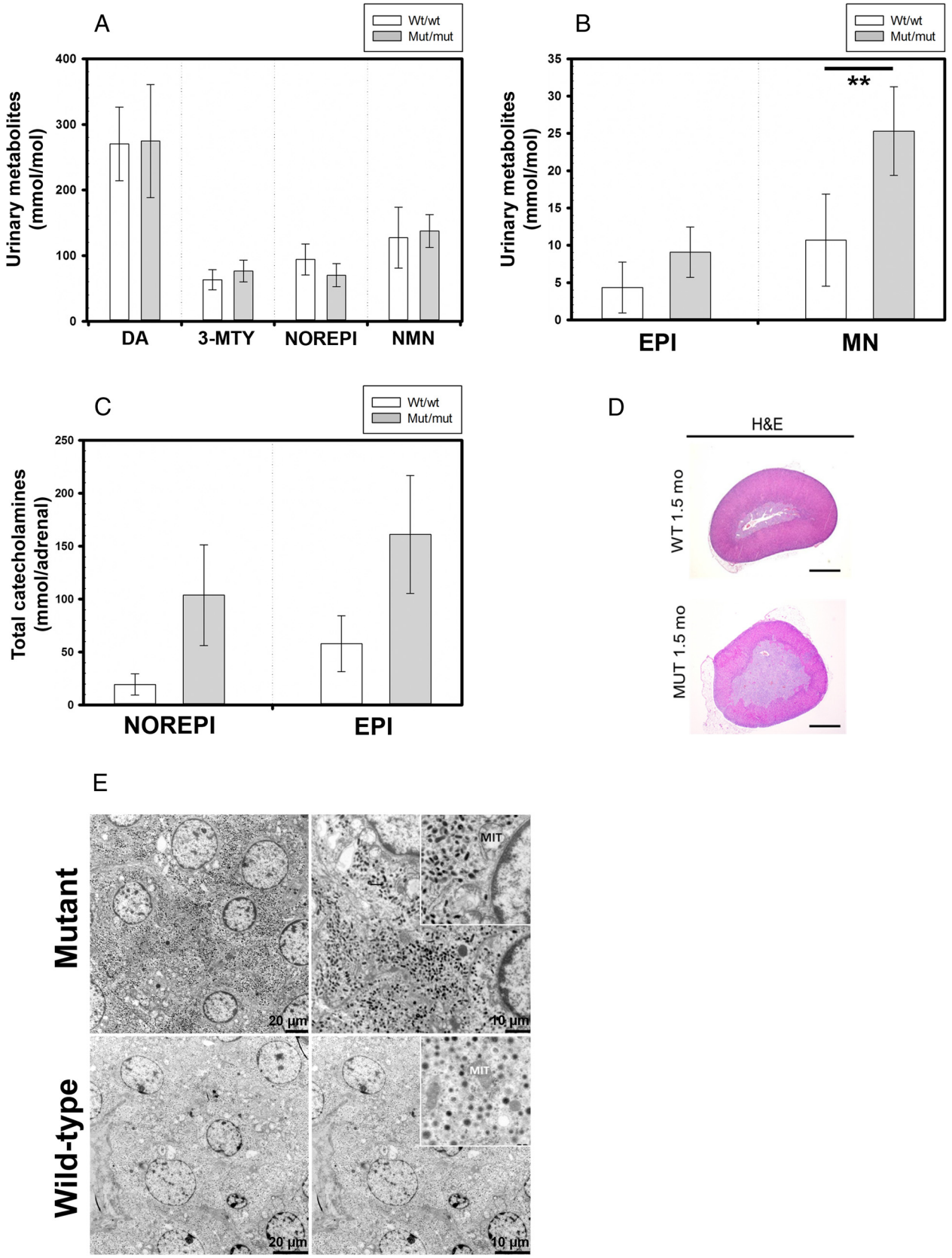

Figure 2. Catecholamine levels, adrenal gland histology and adrenal medulla ultrastructure in young rats. (A, B) Measurement of catecholamine levels in the urine of 1-month-old wild-type (Wt/wt) and mutant (Mut/mut) littermates. Samples were obtained from 19 mutant and 9 wild-type rats. DA, dopamine; 3-MTY, methoxytyramine; NOREPI, norepinephrine; NMN, normetanephrine; EPI, epinephrine; MN, metanephrine. EPI and MN are shown separately due to the different scale. **, $P < .001$. C, Measurement of epinephrine and norepinephrine amount in the adrenal

catecholamines than those of wt animals (Figure 2C). At this stage, the adrenal glands of mutant and wt rats are highly similar in terms of size and weight, but the medulla can be already hyperplastic (Figure 2D).

Altogether, in mutant rats urinary outputs of norepinephrine, normetanephrine and 3-methoxytyramine increase with tumor progression. In contrast, the levels of metanephrine are high at all ages tested already starting at 1 month of age, indicating that this phenotype is genetically determined.

In agreement with data of catecholamine content, ultrastructural analysis of adrenal chromaffin cells of mutant rats showed that they contain highly elevated numbers of dense core vesicles of ovoid shape, while they seem to lack the moderately electron-dense vesicles of rounded shape seen in the cells of wt rats (Figure 2E).

Immunohistochemistry

The adrenal medulla of rodents contains two cell populations of adrenergic and noradrenergic chromaffin cells that can be distinguished based on the expression of the enzyme phenylethanolamine *N*-methyltransferase (PNMT), which is expressed only in the former cell type. We previously reported that the tumors in MENX rats are not immunoreactive to the anti-PNMT antibody (24). We here analyzed the adrenal glands of mutant and wt rats at the ages also employed for the biochemical and ultrastructural analyses, ie, at 1.5, 4, 6 and 8 months. Representative stainings are shown in Figure 3.

These stainings show that from a very early age (1.5 months) the mutant rats have a higher proportion of PNMT-negative cells than the wt animals (Figure 3). With age (ie, with tumor progression), the amount of PNMT-negative cells in the mutant rats increases significantly (Figure 3). Given that in wt rats no changes in adrenal gland morphology and PNMT expression were observed between the 6 and the 8 month time points, we only show the PNMT staining of a representative 8 months old mutant animal.

Pathophysiology

The most common sign of PCC is hypertension, found in most patients with symptomatic disease and resulting from increases in circulating catecholamines (32). To determine whether the high levels of excreted norepinephrine in MENX rats with PCC associate with hypertension, we measured longitudinally and noninvasively systolic BP in a series of mutant (n = 7) and wt (n = 5) rats of both genders at ages of 4, 6 and 8 months. Given minimal association of gender with BP differences, the data from males and females of each genotype were combined. We observed that BP was significantly elevated in mutant rats at 4 months of age compared to age-matched wt animals ($P = .0017$), and remained elevated at all subsequent ages (Figure 4). By 8 months of age, the mutant rats show on average a 57% increase in BP compared to wt age-matched animals (107.2 ± 3.3 mmHg; 168.1 ± 30.6 mmHg; $P = .0016$).

Persistent high BP in patients with PCC, if left uncontrolled, can cause damage to several organs and tissues, including arteries, heart, and kidneys (33–36). To determine the effects of hypertension in MENX-affected rats, we analyzed heart and kidney tissues at various ages using different histological staining procedures. In the myocardium of mutant rats older than 6 months of age we observed a profusion of cells with elongated nuclei (Anitschkow- or caterpillar-like cells) and a thickening of blood vessel walls (Figure 5 A,B). Using Periodic acid-Schiff (PAS) staining to detect proteoglycans in the basal membrane of blood vessels, a general disorganization of the cell layers around the blood vessel wall can be appreciated (Figure 5 C). Tissue scarring was also present. Elastica–Van Gieson trichrome staining revealed perivascular fibrosis extending into the surrounding of the blood vessels (Figure 5 D). These phenotypes were not seen in the myocardium of wild-type rats up to 8 months of age (data not shown).

The kidneys of mutant rats 6 months and older showed accumulation of proteins in the ducts and thickening of the Bowmann's capsule (Figure 5E). Additionally, all mutant rats showed severe proteinuria (x ≥ 500 mg/dl) (data not shown). Evidence of glomerular damage was apparent from the presence of both hyperplastic and hypoplastic glomeruli, with the occasional appearance of necrotic cells. Recruitment of inflammatory cells was also observed in mutant rat kidneys (Figure 5F). Altogether, the pathological changes observed in the mutant rats are consistent with renal damage caused by sustained high BP. Wt rats showed no pathological changes in the kidneys up to 8 months of age (data not shown).

Legend to Figure 2 Continued. . .
gland tissues of 1-month-old Wt/wt (n = 5) and Mut/mut rats (n = 4). The results are the average of the catecholamine content per adrenal gland. D, Hematoxylin & eosin (H&E) staining of the adrenal glands of 1,5-month-old wild-type (WT) and mutant (MUT) littermates. Original magnification: 20×; bar, 500 μm. E, Ultrastructural analysis of adrenal medullary cells in 1-month-old Wt/wt and Mut/mut rats. MIT, mitochondria.

Discussion

PCCs are tumors of the adrenal medulla characterized by production of catecholamines leading to increased BP with associated end-organ pathology. Lack of suitable animal models for PCC has presented an obstacle for preclinical studies directed at elucidating the pathophysiology or developing new therapies for these tumors. Here we characterize a spontaneous animal model (MENX) that develops PCC with complete penetrance. We show that this model displays morphological and biochemical features of the tumor with increases in BP and development of end-organ pathology that recapitulate the clinical characteristics of PCC.

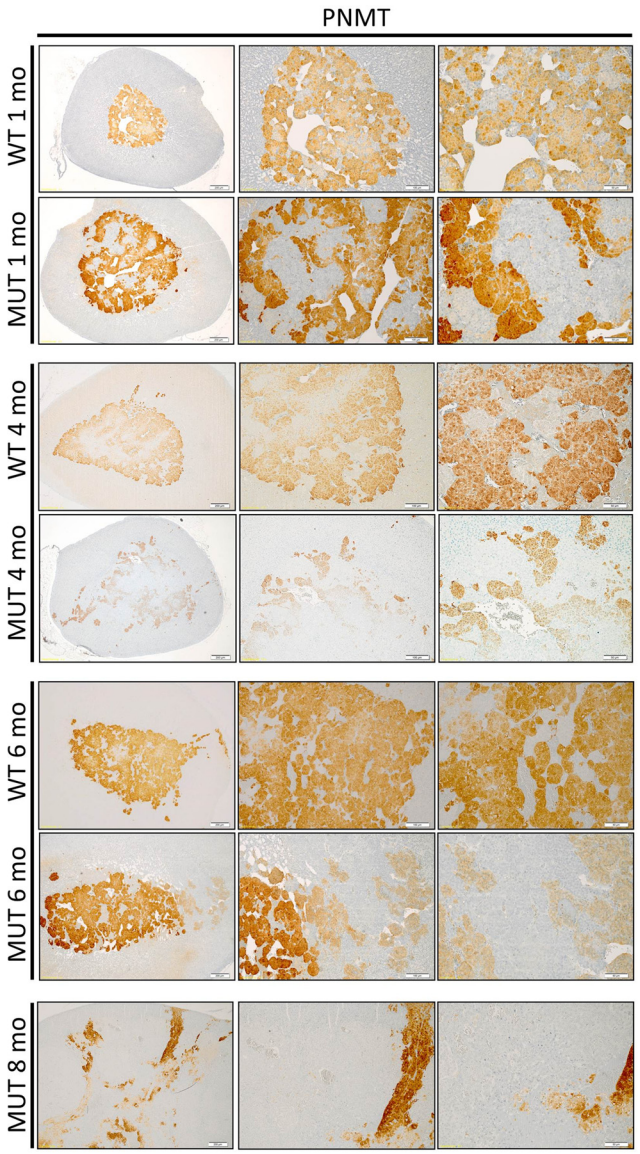

Figure 3. Expression of PNMT in the adrenal glands of wild-type (WT) and mutant (MUT) rats at different ages. Original magnifications were: X40 (left panels); x100 (central panels); x200 (right panels).

As now demonstrated, the MENX model is characterized by development of tumors that produce increases in predominantly urinary norepinephrine and its O-methylated metabolite, normetanephrine. Additionally, in mu-

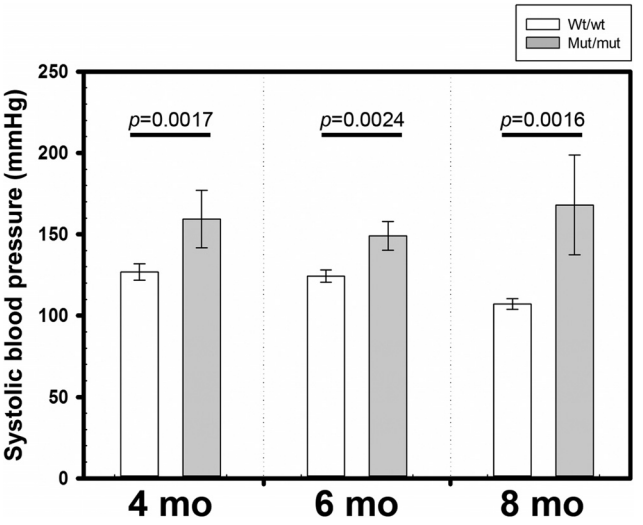

Figure 4. Systolic BP in the same wild-type (Wt/wt) and mutant (Mut/mut) rats analyzed at different ages. Noninvasive tail-cuff measurements were obtained from 5 Wt/wt and 10 Mut/mut rats. Mo, months.

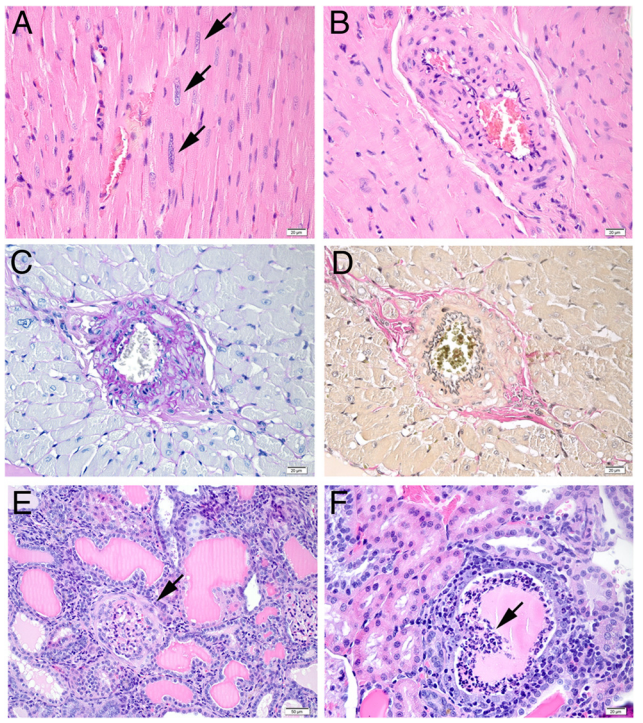

Figure 5. Histological analysis of heart (A-D) and kidney (E,F) tissues of homozygous mutant rats at age > 6 months. (A,B) Hematoxilin & eosin (H&E) staining of myocardium. The arrows point to Anitschkow- or caterpillar-like" cells. C, PAS staining specific for proteoglycans of a myocardial blood vessel. D, Elastica-Van Gieson trichrome staining of the same vessel shown in panel C showing perivascular fibrosis. (E,F) H&E staining of the kidney. E, Protein casts are visible in the ducts. The arrow points to the thickening of the Bowmann's capsule. F, Necrosis of the glomerular tuft.

tant rats we observed an age-independent substantial elevation of urinary metanephrine, the O-methylated metabolite of epinephrine, already at 1 month of age, well before development of tumor nodules. Lack of parallel age-related increases in urinary excretion of dopamine with increases in its O-methylated metabolite, methoxytyramine, presumably reflects different sources of these amines; in particular, most urinary dopamine in both humans and rats is derived from renal decarboxylation of circulating L-dopa rather than extraction of circulating dopamine (37–39). Thus, as in patients with PCC (40), measurements of methoxytyramine provide a more reliable indicator of tumoral dopamine production than urinary dopamine.

Similar to the situation for methoxytyramine and dopamine, but for largely different reasons, measurements of metanephrine provide a more reliable indicator of tumoral or chromaffin cell epinephrine synthesis than measurements of epinephrine itself. Metanephrine is produced largely from epinephrine leaking from storage vesicles of adrenal medullary cells and thereby reflects the size of chromaffin cell epinephrine stores (41–43). The substantially elevated urinary excretion of metanephrine in MENX compared to wt rats at an early age (ie, before development of predominantly norepinephrine-producing tumors) thus reflects increased stores of adrenal medullary epinephrine. Lack of parallel increases in urine epinephrine reflects dissociation of epinephrine exocytotic secretion from epinephrine synthesis, storage and metabolism as described elsewhere (44).

By immunohistochemical staining for phenylethanolamine N-methyltransfase (PNMT) two populations of chromaffin cells were discerned at all ages in both wt and MENX mutant rat adrenals, a finding consistent with previous observations of two populations of epinephrine- and norepinephrine-producing chromaffin cells in rats (45). From the biochemical and immunohistochemical findings it can be concluded that despite a background of enhanced chromaffin cell epinephrine production, the chromaffin cell tumors that develop in MENX mutant rats lack PNMT and produce mainly, if not exclusively, norepinephrine. Altogether, it seems that the noradrenergic PNMT-negative tumor nodules, responsible for the age-dependent increase in urinary norepinephrine and normetanephrine, develop on a background of adrenal medullary hyperplasia involving increased adrenal medullary contents of epinephrine and production of metanephrine.

Among patients with PCC, those tumors that produce exclusively dopamine, norepinephrine or both catecholamines show distinctly different global patterns of gene expression than those that additionally produce epinephrine (4, 46, 47). The former have been termed Cluster 1 tumors and form in patients with predisposing gene mutations that differ from those leading to epinephrine-producing Cluster 2 tumors (46, 47). Norepinephrine producing Cluster 1 PCCs secrete the catecholamines more continuously than epinephrine-producing tumors, reflecting a more immature secretory phenotype with less control to restrict exocytosis (44, 48). This is also consistent with the norepinephrine-producing PCCs in MENX mutant rats in which elevated urinary excretion of norepinephrine was associated with consistent elevations of BP at all measured time points compared to wt rats.

In mutant rats, PCC-related organ-specific hypertensive complications were also found that closely resemble the lesions among patients with these tumors. Vasoconstriction, resulting from the action of catecholamines on α-adrenergic receptors and leading to high BP, forces the heart to work harder than necessary to pump blood to provide adequate organ perfusion. Moreover, high levels of circulating catecholamines may directly contribute to end-organ pathology by structurally changing the vasculature and increasing extracellular matrix proteins, including collagen and fibronectin (33). Catecholamines can also exert direct toxic effects on the myocardium and directly promote hypertrophy, further contributing to the severe cardiovascular complications of pheochromocytoma (49). In the MENX model, pathological changes included thickening of the blood vessels, myocardial fibroses and myocardial hypertrophy, all features also observed in patients with PCC (49).

In addition to pathological changes in the heart, we also observed pathological changes in the kidneys of mutant rats. These included protein casts in the ducts due to both vascular stiffening and damage to the basal lamina of the filtration barrier, likely caused by elevated BP. Additionally, necrosis of the glomerular tuft could be demonstrated, again probably caused by sustained high BP, with subsequent hypoperfusion and resulting hypoxia. These are changes consistent with those previously reported in the kidneys of patients with endocrine forms of secondary hypertension (50). While the end-organ pathological findings in mutant rats reported here are consistent with changes associated with high BP in human PCC patients, we cannot formally exclude that some of these phenotypes might be related to the genetic mutation in p27. Mice defective for p27 (p27-/-) develop pheochromocytoma in 23.8% of cases (51). In these mice, no pathological alterations similar to those we observed in MENX mutant rats have been reported (51), however the number of animals analyzed was low.

In summary, the MENX rat model recapitulates the most relevant pathophysiological features of human PCC.

Since, similar to human patients, MENX rats are characterized by increased catecholamine secretion and sustained hypertension, they provide a promising model for elucidating the pathophysiology of PCC and for preclinical and translational studies aimed at developing novel targeted therapies for these tumors.

Acknowledgments

We dedicate this article to the memory of Dr. Monika Ehrhart-Bornstein. We thank D. Mörzl and E.Pulz for technical assistance. This work was supported by grants SFB824, subproject B08, from the Deutsche Forschungsgemeinschaft (DFG) and grant #110874 from the Deutsche Krebshilfe (to N.S.P.). N.S.P. was appointed to the "Eleonore Trefftz Program for Visiting Women Professors" at the Technical University Dresden.

Address all correspondence and requests for reprints to: Natalia S. Pellegata, PhD, Institute of Pathology, Helmholtz Zentrum München, Ingolstaedter Landstrasse 1, 85 764 Neuherberg, Germany, Tel.: 089–3187 2633, FAX: 089–3187 3360, e-mail: natalia.pellegata@helmholtz-muenchen.de

Disclosure Summary: The authors have nothing to disclose.
This work was supported by .

References

1. **Moraitis AG, Martucci VL, Pacak K.** Genetics, diagnosis, and management of medullary thyroid carcinoma and pheochromocytoma/paraganglioma. *Endocr Pract*. 2014;20:176–87.
2. **Castro-Vega LJ, Letouze E, Burnichon N, Buffet A, Disderot PH, Khalifa E, Loriot C, Elarouci N, Morin A, Menara M, Lepoutre-Lussey C, Badoual C, Sibony M, Dousset B, Libe R, Zinzindohoue F, Plouin PF, Bertherat J, Amar L, de Reynies A, Favier J, Gimenez-Roqueplo AP.** Multi-omics analysis defines core genomic alterations in pheochromocytomas and paragangliomas. *Nat Commun*. 2015;6:6044.
3. **Fishbein L, Khare S, Wubbenhorst B, DeSloover D, D'Andrea K, Merrill S, Cho NW, Greenberg RA, Else T, Montone K, LiVolsi V, Fraker D, Daber R, Cohen DL, Nathanson KL.** Whole-exome sequencing identifies somatic ATRX mutations in pheochromocytomas and paragangliomas. *Nat Commun*. 2015;6:6140.
4. **Eisenhofer G, Huynh TT, Pacak K, Brouwers FM, Walther MM, Linehan WM, Munson PJ, Mannelli M, Goldstein DS, Elkahloun AG.** Distinct gene expression profiles in norepinephrine- and epinephrine-producing hereditary and sporadic pheochromocytomas: activation of hypoxia-driven angiogenic pathways in von Hippel-Lindau syndrome. *Endocr Relat Cancer*. 2004;11:897–911.
5. **Lopez-Jimenez E, Gomez-Lopez G, Leandro-Garcia LJ, Munoz I, Schiavi F, Montero-Conde C, de Cubas AA, Ramires R, Landa I, Leskela S, Maliszewska A, Inglada-Perez L, de la Vega L, Rodriguez-Antona C, Leton R, Bernal C, de Campos JM, Diez-Tascon C, Fraga MF, Boullosa C, Pisano DG, Opocher G, Robledo M, Cascon A.** Research resource: Transcriptional profiling reveals different pseudohypoxic signatures in SDHB and VHL-related pheochromocytomas. *Mol Endocrinol*. 2010;24:2382–2391.
6. **Ayala-Ramirez M, Feng L, Johnson MM, Ejaz S, Habra MA, Rich T, Busaidy N, Cote GJ, Perrier N, Phan A, Patel S, Waguespack S, Jimenez C.** Clinical risk factors for malignancy and overall survival in patients with pheochromocytomas and sympathetic paragangliomas: primary tumor size and primary tumor location as prognostic indicators. *J Clin Endocrinol Metab*. 2011;96:717–725.
7. **Eisenhofer G, Bornstein SR, Brouwers FM, Cheung NK, Dahia PL, de Krijger RR, Giordano TJ, Greene LA, Goldstein DS, Lehnert H, Manger WM, Maris JM, Neumann HP, Pacak K, Shulkin BL, Smith DI, Tischler AS, Young WF, Jr.** Malignant pheochromocytoma: current status and initiatives for future progress. *Endocr Relat Cancer*. 2004;11:423–436.
8. **Loh KC, Fitzgerald PA, Matthay KK, Yeo PP, Price DC.** The treatment of malignant pheochromocytoma with iodine-131 metaiodobenzylguanidine (131I-MIBG): a comprehensive review of 116 reported patients. *J Endocrinol Invest*. 1997;20:648–658.
9. **Joshua AM, Ezzat S, Asa SL, Evans A, Broom R, Freeman M, Knox JJ.** Rationale and evidence for sunitinib in the treatment of malignant paraganglioma/pheochromocytoma. *J Clin Endocrinol Metab*. 2009;94:5–9.
10. **Druce MR, Kaltsas GA, Fraenkel M, Gross DJ, Grossman AB.** Novel and evolving therapies in the treatment of malignant phaeochromocytoma: experience with the mTOR inhibitor everolimus (RAD001). *Horm Metab Res*. 2009;41:697–702.
11. **Oh DY, Kim TW, Park YS, Shin SJ, Shin SH, Song EK, Lee HJ, Lee KW, Bang YJ.** Phase 2 study of everolimus monotherapy in patients with nonfunctioning neuroendocrine tumors or pheochromocytomas/paragangliomas. *Cancer*. 2012;118:6162–6170.
12. **Nikitin AY, Juarez-Perez MI, Li S, Huang L, Lee WH.** RB-mediated suppression of spontaneous multiple neuroendocrine neoplasia and lung metastases in Rb+/- mice. *Proc Natl Acad Sci U S A*. 1999;96:3916–3921.
13. **Tonks ID, Mould AW, Schroder WA, Cotterill A, Hayward NK, Walker GJ, Kay GF.** Dual loss of rb1 and Trp53 in the adrenal medulla leads to spontaneous pheochromocytoma. *Neoplasia*. 2010;12:235–243.
14. **Jacks T, Shih TS, Schmitt EM, Bronson RT, Bernards A, Weinberg RA.** Tumour predisposition in mice heterozygous for a targeted mutation in Nf1. *Nat Genet*. 1994;7:353–361.
15. **Franklin DS, Godfrey VL, O'Brien DA, Deng C, Xiong Y.** Functional collaboration between different cyclin-dependent kinase inhibitors suppresses tumor growth with distinct tissue specificity. *Mol Cell Biol*. 2000;20:6147–6158.
16. **Di Cristofano A, De Acetis M, Koff A, Cordon-Cardo C, Pandolfi PP.** Pten and p27KIP1 cooperate in prostate cancer tumor suppression in the mouse. *Nat Genet*. 2001;27:222–224.
17. **Powers JF, Evinger MJ, Tsokas P, Bedri S, Alroy J, Shahsavari M, Tischler AS.** Pheochromocytoma cell lines from heterozygous neurofibromatosis knockout mice. *Cell Tissue Res*. 2000;302:309–320.
18. **Martiniova L, Lai EW, Elkahloun AG, Abu-Asab M, Wickremasinghe A, Solis DC, Perera SM, Huynh TT, Lubensky IA, Tischler AS, Kvetnansky R, Alesci S, Morris JC, Pacak K.** Characterization of an animal model of aggressive metastatic pheochromocytoma linked to a specific gene signature. *Clin Exp Metastasis*. 2009;26:239–250.
19. **Ullrich M, Bergmann R, Peitzsch M, Cartellieri M, Qin N, Ehrhart-Bornstein M, Block NL, Schally AV, Pietzsch J, Eisenhofer G, Bornstein SR, Ziegler CG.** In vivo fluorescence imaging and urinary monoamines as surrogate biomarkers of disease progression in a mouse model of pheochromocytoma. *Endocrinology*. 2014;155:4149–4156.
20. **Pacak K, Sirova M, Giubellino A, Lencesova L, Csaderova L, Laukova M, Hudecova S, Krizanova O.** NF-kappaB inhibition significantly upregulates the norepinephrine transporter system, causes apoptosis in pheochromocytoma cell lines and prevents metastasis in an animal model. *Int J Cancer*. 2012;131:2445–2455.
21. **Nolting S, Giubellino A, Tayem Y, Young K, Lauseker M, Bullova P, Schovanek J, Anver M, Fliedner S, Korbonits M, Goke B, Vlotides G, Grossman A, Pacak K.** Combination of 13-Cis retinoic acid and lovastatin: marked antitumor potential in vivo in a pheochromocy-

toma allograft model in female athymic nude mice. *Endocrinology*. 2014;155:2377–2390.
22. **Molatore S, Pellegata NS.** The MENX syndrome and p27: relationships with multiple endocrine neoplasia. *Prog Brain Res*. 2010;182:295–320.
23. **Shyla A, Holzlwimmer G, Calzada-Wack J, Bink K, Tischenko O, Guilly MN, Chevillard S, Samson E, Graw J, Atkinson MJ, Pellegata NS.** Allelic loss of chromosomes 8 and 19 in MENX-associated rat pheochromocytoma. *Int J Cancer*. 2010;126:2362–2372.
24. **Molatore S, Liyanarachchi S, Irmler M, Perren A, Mannelli M, Ercolino T, Beuschlein F, Jarzab B, Wloch J, Ziaja J, Zoubaa S, Neff F, Beckers J, Hofler H, Atkinson MJ, Pellegata NS.** Pheochromocytoma in rats with multiple endocrine neoplasia (MENX) shares gene expression patterns with human pheochromocytoma. *Proc Natl Acad Sci U S A*. 2010;107:18493–18498.
25. **Miederer M, Molatore S, Marinoni I, Perren A, Spitzweg C, Reder S, Wester HJ, Buck AK, Schwaiger M, Pellegata NS.** Functional Imaging of Pheochromocytoma with Ga-DOTATOC and C-HED in a Genetically Defined Rat Model of Multiple Endocrine Neoplasia. *Int J Mol Imaging*. 2011;2011:175352.
26. **Gaertner FC, Wiedemann T, Yousefi BH, Lee M, Repokis I, Higuchi T, Nekolla SG, Yu M, Robinson S, Schwaiger M, Pellegata NS.** Preclinical evaluation of 18F-LMI1195 for in vivo imaging of pheochromocytoma in the MENX tumor model. *J Nucl Med*. 2013;54:2111–2117.
27. **Fritz A, Walch A, Piotrowska K, Rosemann M, Schaffer E, Weber K, Timper A, Wildner G, Graw J, Hofler H, Atkinson MJ.** Recessive transmission of a multiple endocrine neoplasia syndrome in the rat. *Cancer Res*. 2002;62:3048–3051.
28. **Langer R, Von Rahden BH, Nahrig J, Von Weyhern C, Reiter R, Feith M, Stein HJ, Siewert JR, Hofler H, Sarbia M.** Prognostic significance of expression patterns of c-erbB-2, p53, p16INK4A, p27KIP1, cyclin D1 and epidermal growth factor receptor in oesophageal adenocarcinoma: a tissue microarray study. *J Clin Pathol*. 2006;59:631–634.
29. **Peitzsch M, Pelzel D, Glockner S, Prejbisz A, Fassnacht M, Beuschlein F, Januszewicz A, Siegert G, Eisenhofer G.** Simultaneous liquid chromatography tandem mass spectrometric determination of urinary free metanephrines and catecholamines, with comparisons of free and deconjugated metabolites. *Clin Chim Acta*. 2013;418:50–58.
30. **Eisenhofer G, Goldstein DS, Stull R, Keiser HR, Sunderland T, Murphy DL, Kopin IJ.** Simultaneous liquid-chromatographic determination of 3,4-dihydroxyphenylglycol, catecholamines, and 3,4-dihydroxyphenylalanine in plasma, and their responses to inhibition of monoamine oxidase. *Clin Chem*. 1986;32:2030–2033.
31. **Hoelter SM, Dalke C, Kallnik M, Becker L, Horsch M, Schrewe A, Favor J, Klopstock T, Beckers J, Ivandic B, Gailus-Durner V, Fuchs H, Hrabe de Angelis M, Graw J, Wurst W.** "Sighted C3H" mice–a tool for analysing the influence of vision on mouse behaviour? *Front Biosci*. 2008;13:5810–5823.
32. **Calhoun DA, Jones D, Textor S, Goff DC, Murphy TP, Toto RD, White A, Cushman WC, White W, Sica D, Ferdinand K, Giles TD, Falkner B, Carey RM.** Resistant hypertension: diagnosis, evaluation, and treatment. A scientific statement from the American Heart Association Professional Education Committee of the Council for High Blood Pressure Research. *Hypertension*. 2008;51:1403–1419.
33. **O'Callaghan CJ, Williams B.** The regulation of human vascular smooth muscle extracellular matrix protein production by alpha- and beta-adrenoceptor stimulation. *J Hypertens*. 2002;20:287–294.
34. **Brouwers FM, Lenders JW, Eisenhofer G, Pacak K.** Pheochromocytoma as an endocrine emergency. *Rev Endocr Metab Disord*. 2003;4:121–128.
35. **Hill FS, Jander HP, Murad T, Diethelm AG.** The coexistence of renal artery stenosis and pheochromocytoma. *Ann Surg*. 1983;197:484–490.
36. **Crowe AV, Jones NF, Carr P.** Five ways to be fooled by phaeochromocytoma–renal and urological complications. *Nephrol Dial Transplant*. 1997;12:337–340.
37. **Brown MJ, Allison DJ.** Renal conversion of plasma DOPA to urine dopamine. *Br J Clin Pharmacol*. 1981;12:251–253.
38. **Grossman E, Hoffman A, Armando I, Abassi Z, Kopin IJ, Goldstein DS.** Sympathoadrenal contribution to plasma dopa (3,4-dihydroxyphenylalanine) in rats. *Clin Sci (Lond)*. 1992;83:65–74.
39. **Wolfovitz E, Grossman E, Folio CJ, Keiser HR, Kopin IJ, Goldstein DS.** Derivation of urinary dopamine from plasma dihydroxyphenylalanine in humans. *Clin Sci (Lond)*. 1993;84:549–557.
40. **Eisenhofer G, Goldstein DS, Sullivan P, Csako G, Brouwers FM, Lai EW, Adams KT, Pacak K.** Biochemical and clinical manifestations of dopamine-producing paragangliomas: utility of plasma methoxytyramine. *J Clin Endocrinol Metab*. 2005;90:2068–2075.
41. **Eisenhofer G, Rundquist B, Aneman A, Friberg P, Dakak N, Kopin IJ, Jacobs MC, Lenders JW.** Regional release and removal of catecholamines and extraneuronal metabolism to metanephrines. *J Clin Endocrinol Metab*. 1995;80:3009–3017.
42. **De Galan BE, Tack CJ, Willemsen JJ, Sweep CG, Smits P, Lenders JW.** Plasma metanephrine levels are decreased in type 1 diabetic patients with a severely impaired epinephrine response to hypoglycemia, indicating reduced adrenomedullary stores of epinephrine. *J Clin Endocrinol Metab*. 2004;89:2057–2061.
43. **Eisenhofer G, Kopin IJ, Goldstein DS.** Catecholamine metabolism: a contemporary view with implications for physiology and medicine. *Pharmacol Rev*. 2004;56:331–349.
44. **Eisenhofer G, Pacak K, Huynh TT, Qin N, Bratslavsky G, Linehan WM, Mannelli M, Friberg P, Grebe SK, Timmers HJ, Bornstein SR, Lenders JW.** Catecholamine metabolomic and secretory phenotypes in phaeochromocytoma. *Endocr Relat Cancer*. 2011;18:97–111.
45. **Phillips JK, Dubey R, Sesiashvilvi E, Takeda M, Christie DL, Lipski J.** Differential expression of the noradrenaline transporter in adrenergic chromaffin cells, ganglion cells and nerve fibres of the rat adrenal medulla. *J Chem Neuroanat*. 2001;21:95–104.
46. **Dahia PL, Ross KN, Wright ME, Hayashida CY, Santagata S, Barontini M, Kung AL, Sanso G, Powers JF, Tischler AS, Hodin R, Heitritter S, Moore F, Dluhy R, Sosa JA, Ocal IT, Benn DE, Marsh DJ, Robinson BG, Schneider K, Garber J, Arum SM, Korbonits M, Grossman A, Pigny P, Toledo SP, Nose V, Li C, Stiles CD.** A HIF1alpha regulatory loop links hypoxia and mitochondrial signals in pheochromocytomas. *PLoS Genet*. 2005;1:72–80.
47. **Qin N, de Cubas AA, Garcia-Martin R, Richter S, Peitzsch M, Menschikowski M, Lenders JW, Timmers HJ, Mannelli M, Opocher G, Economopoulou M, Siegert G, Chavakis T, Pacak K, Robledo M, Eisenhofer G.** Opposing effects of HIF1alpha and HIF2alpha on chromaffin cell phenotypic features and tumor cell proliferation: Insights from MYC-associated factor X. *Int J Cancer*. 2014;135:2054–2064.
48. **Eisenhofer G, Huynh TT, Elkahloun A, Morris JC, Bratslavsky G, Linehan WM, Zhuang Z, Balgley BM, Lee CS, Mannelli M, Lenders JW, Bornstein SR, Pacak K.** Differential expression of the regulated catecholamine secretory pathway in different hereditary forms of pheochromocytoma. *Am J Physiol Endocrinol Metab*. 2008;295:E1223–1233.
49. **Prejbisz A, Lenders JW, Eisenhofer G, Januszewicz A.** Cardiovascular manifestations of phaeochromocytoma. *J Hypertens*. 2011;29:2049–2060.
50. **O'Neal LW, Kissane JM, Hartroft PM.** The kidney in endocrine hypertension. Cushing's syndrome, pheochromocytoma, and aldosteronism. *Arch Surg*. 1970;100:498–505.
51. **Franklin DS1, Godfrey VL, O'Brien DA, Deng C, Xiong Y.** Functional collaboration between different cyclin-dependent kinase inhibitors suppresses tumor growth with distinct tissue specificity. *Mol Cell Biol*. 2000;20:6147–58.